**PAPER**

# Printed fabric heater based on Ag nanowire/carbon nanotube composites

# IOP ebooks™

Bringing you innovative digital publishing with leading voices to create your essential collection of books in STEM research.

Start exploring the collection - download the first chapter of every title for free.

# Printed fabric heater based on Ag nanowire/carbon nanotube composites

**Junseong Ahn[1,2], Jimin Gu[1], Boyeon Hwang[2], Hyeokjung Kang[2], Soonhyoung Hwang[2], Sohee Jeon[2], Junho Jeong[2,3]** and **Inkyu Park[1,3]**

[1] Department of Mechanical Engineering, Korea Advanced Institute of Science and Technology (KAIST), Daejeon 34141, Republic of Korea
[2] Department of Nano Manufacturing Technology, Korea Institute of Machinery and Materials (KIMM), Daejeon 34103, Republic of Korea

E-mail: jhjeong@kimm.re.kr and inkyu@kaist.ac.kr

## Abstract

The increasing demand for smart fabrics has inspired extensive research in the field of nanomaterial-based wearable heaters. However, existing stretchable heaters employ polymer substrates, and hence require additional substrate-fabric bonding that can result in high thermal contact resistance. Moreover, currently used stretchable fabric heaters suffer from high sheet resistance and require complex fabrication processes. In addition, conventional fabrication methods do not allow for patternability, thus hindering the fabrication of wearable heaters with diverse designs. Herein, we propose an improved spray coating method well suited for the preparation of patternable heaters on commercial fabrics, combining the structural stability of carbon nanotubes with the high electrical conductivity of Ag nanowires to fabricate a stretchable fabric heater with excellent mechanical (stretchability $\approx 50\%$) and electrical (sheet resistance $\approx 22\,\Omega\,\text{sq}^{-1}$) properties. The fabricated wearable heater reaches typical operating temperatures of 35 °C–55 °C at a low driving voltage of 3–5 V with a proper surface power density of 26.6–72.2 mW cm$^{-2}$ (heater area: 3 cm × 3 cm) and maintains a stable heating temperature for more than 30 h. This heater shows a stable performance even when folded or rolled, thus being well suited for the practical wearable applications.

Supplementary material for this article is available online

(Some figures may appear in colour only in the online journal)

## 1. Introduction

Recent technological advances have resulted in an increased demand for smart textiles, which are widely used in medical and healthcare, sport and fitness, protection and safety, and military applications [1]. Moreover, smart textiles have found diverse applications in organic solar cells, thermoelectric and piezoelectric devices, electrochemical energy storage devices, and chromatic and actuating devices [2]. In particular, smart textile-based functional fabric heaters are expected to find numerous real-life applications, such as automobile defrosting, temperature preservation, thermal therapy, and controlled drug delivery, and have therefore been widely investigated [3–6]. For such heaters to be practically applicable, they must exhibit high stretchability, flexibility, portability, body conformability, patternability, and low power consumption. Polymer-nanocomposite [7–25] film heaters comprising flexible and conductive nanomaterials, such as graphene [13, 14], carbon nanotubes (CNTs) [15–17], and metal nanowires (NWs) [18–25], as well as polymers, such as polydimethylsiloxane (PDMS) and polyethylene terephthalate (PET), meet the abovementioned requirements but exhibit the

---

[3] Authors to whom any correspondence should be addressed.

inevitable disadvantage of additional thermal contact resistance as they must be additionally attached to clothing when used. Although this thermal contact problem can be solved by the use of sewable conductive threads, such as graphene fibers [26], conductive polymers [27], and CNTs/graphene composite [28], this approach has certain fundamental limitations such as strain-induced rapid resistance change and high electrical resistance of polymer.

The abovementioned limitations have triggered numerous studies on the direct deposition of nanomaterials onto commercial fabrics as a way of circumventing the problem of additional thermal contact resistance. Unfortunately, unlike in the case of polymer-nanocomposite film heaters, the technology of nanomaterial-based fabric heater fabrication is still limited by the narrow choice of heating materials and coating methods. Generally, CNTs [29] and poly(3,4-ethylenedioxythiophene) [3, 30–32] are frequently selected as conductive materials because of their excellent mechanical strength/ electrical conductivity and good adhesion to the fabric substrate. However, these materials require high driving voltages and exhibit low stretchability. In addition, dip coating [3, 4, 29, 33], which is most widely used because of the nonuniformity and high roughness of the fabric surface, does not allow patterning on fabric and consequently requires the entire cloth to be used as a heater. Consequently, the dip-coating method cannot be applied to the fabrication of fabric heaters with diverse designs. The same problems are also observed for other methods such as polymerization [31, 32, 34]. Although there are some exceptions, such as physical vapor deposition [35] and dip-coating of thread [5], which can make patterns with a shadow mask or weaving, these are not very efficient method. The former requires high vacuum equipment for deposition and the latter requires sewing process of dip-coated threads. Recently, Zhang *et al* [6] developed a carbonization method and employed a weft-knitted fabric structure to fabricate a heater with low electrical resistance and high stretchability; unfortunately, this method necessitates the use of high temperature (>1000 °C) and does not allow patterning. Therefore, the fabrication of fabric heaters with high stretchability, patternability, body conformability, flexibility, low driving voltage, and stable performance remains challenging.

Herein, we solve the abovementioned issues and fabricate a high-performance fabric heater by direct spray coating of CNTs/Ag NWs onto a fabric and realize patterning in a several-millimeter scale by using a shadow mask (figure S1 is available online at stacks.iop.org/NANO/30/455707/ mmedia). In particular, CNTs were used as the main structural material to improve the network structure and mechanical stability, while Ag NWs were used as a supporting material to increase the electrical conductivity [8, 10, 12, 24, 36, 37]. The polymer-encapsulated fabric heater maintained a stable temperature even when folded or rolled, and long-term performance testing revealed that a stable state could be maintained without any temperature change for more than 30 h at high temperature (100 °C). In addition, the whole fabrication process was performed at room temperature in the absence of special chemical

treatment and costly facilities, and was found to be suitable for large-scale low-cost production. Finally, the developed technique was used to fabricate a flexible heater on commercial cotton gloves as well as a flexible and portable defrosting heater.

## 2. Experimental

### 2.1. Preparation of the coating solution (CNT/Ag NW)

Multi-walled CNTs (Hanwha, Korea) were mixed with isopropyl alcohol (IPA; Sigma Aldrich Korea, Korea) to achieve a loading of 0.02 wt%, and the resulting mixture was subjected to sonication for 10 min (VCX-130 tip sonicator, Sonics and Materials, USA). The sonication process comprised a series of 3 s injections followed by 1 s rest periods to prevent the thermally induced aggregation of CNTs. The obtained solution was treated with Ag NWs solution (UniNano Tech, Korea) and deionized (DI) water to achieve a NW loading of 0.02 wt%, sonicated for 5 min as described earlier, and allowed to cool to room temperature over 30 min.

### 2.2. Preparation of the fabric heater

The dispersion obtained earlier was spray coated using a spray coater (EFD 781S, Nordson EFD Korea, Korea; inner diameter of nozzle = 1.17 mm) on a 3 cm × 3 cm × 0.02 cm piece of stretchable fabric substrate (80% nylon, 20% polyurethane, thickness: 0.2 mm) at a pre-strain of 30% to allow the penetration of conductive nanomaterials into the fabric. A regulator pressure of 0.05 MPa and a round-pattern nozzle (#7857-46SS, Nordson EFD Korea, Korea) were used. The basic sequence of the coating process corresponded to a 3 s spraying followed by a 10 s waiting period for solvent absorption. An absorbent (cleanroom wiper) was placed under the fabric to absorb solvent residues. To prevent the formation of large cracks and CNT/Ag NW aggregation, the impregnated fabric was oven-dried for 30 min at 50 °C after 15 ml of the solution was spray coated in each cycle (3 cycles and 45 ml of the coating solution was consumed in total, which means 5 ml cm$^{-2}$). During the drying process, intentional cracking was applied using a customized manual linear stage with a fixed strain of 30% for preventing the aggregation of nanomaterials.

After spray coating was completed, the fabric side was fitted with a Cu wire using Ag paste (Dotite D-500, Fujikura Kasei, Japan) as a conductive adhesion material, and the (sample + Cu electrode) assembly was oven-dried at 50 °C for 2 h. Finally, liquid silicone rubber precursors (Ecoflex 00-30, Smooth-On, USA) were poured onto the sample and cured at 50 °C in a convection oven for 1 h. To eliminate air bubbles and mix the precursors, liquid precursors were mixed through centrifugation.

### 2.3. Optimization of the Ag NW:CNT weight ratio

The solution of CNTs in IPA prepared as described in section 2.1 was treated with Ag NWs to achieve Ag NW:CNT

weight ratios of 0:4, 1:3, 2:2, 3:1, and 4:0. For each ratio, 35 ml of the solution was coated, and the prepared samples were characterized through scanning electron microscopy (SEM; Sirion, FEI Co., the Netherlands) and sheet resistance measurements (FPP-2400 four-point probe, Dasol Eng, Korea). For the sheet resistance measurements, five portions of the same sample were examined. The occurrence of millimeter-sized cracks was recorded visually for some samples, which had high degree of CNT aggregation upon the application of 30% strain. The optimized composition of coating solution was identified as 0.02 wt% CNTs and 0.02 wt% Ag NWs; 45 ml of this solution was coated onto the fabric to prepare a heater for further characterization.

### 2.4. Characterization of the fabric heater

During experiments with the fabricated heater (3 cm × 3 cm), the temperature was recorded by a data logger (midi LOGGER GL220, Graphtec, Japan). Strain was applied using a high-precision motorized linear stage, and electrical resistance and current were measured using a source meter (Keithley 2400, Tektronix, USA). As the heater stiffness was too low to allow the use of the linear stage for bending and rolling tests, these tests were performed using PET as a foldable mounting substrate. Voltage was applied utilizing a power supply (UP-3005D, UNICORN TMI, Korea), and infrared (IR) thermal imaging was performed by an IR thermal camera (E6, FLIR Systems, USA).

### 2.5. Heating glove fabrication and defrosting test

A commercial black cotton glove (70% cotton, 30% polyester) was coated with the coating solution (CNT/Ag NW) described earlier. Except for the part to be coated, the glove surface was masked by taping. The Cu wire/Ag paste electrodes and protecting polymer were fabricated, as described in section 2.2, and covered with the same glove fabric as a protective layer. For the defrosting test, a large size fabric heater (4 cm × 3 cm) was fabricated as described in section 2.2. The defrosting test was carried out in a freezer room at an ambient temperature of −15 °C. Frosted glass was placed on the fabric heater (5 cm × 5 cm) and imaged at 30 s intervals after Joule heating by using a DSLR camera (EOS 750D, Canon, Japan). Image analysis was performed using Matlab (MathWorks, USA). Black pixels (defrosted) were represented as 0, while white pixels (frosted) were represented as 1, and intermediate colors were divided by 255. Full defrosting was defined as 0% frost, and the initial state was defined as 100% frost.

## 3. Results and discussion

### 3.1. Preparation of the fabric heater

As mentioned in section 1, general coating methods cannot be easily applied to fabrics because of their nonuniform surface morphologies, i.e. few technologies are currently available for the fabrication of fabric heaters with high stretchability, low driving voltage, and patternability. Therefore, in this study, we resolved the abovementioned problem by modifying the existing spray coating method as well as the materials for coating to make it applicable to fabrics and utilized the developed technique to fabricate a stretchable and patterned fabric heater.

The first improvement from the existing method corresponds to the transfer of nanomaterials onto the fabric and the absorption of solvent flowing to the back of the fabric. In general, spray coating requires continuous drying to prevent the surface of the target material from being wetted by the accumulated solvent or the detachment of already coated nanomaterials [38]. Therefore, we employed a breathable fabric to shorten the drying time and prevent the coating solution from interfering with nanomaterial adhesion. In specific, a clean wiper capable of fast solvent absorption was placed on the back of the fabric to limit the water content in the fabric during the spray coating process. When the sprayed solution reached the fabric substrate, the dispersed nanomaterials adhered to the fabric, while the solvent flowed into the fabric and was absorbed by the wiper, allowing the fabric to be rapidly coated by large amounts of Ag NWs/CNTs.

The second improvement corresponds to the presence of DI water (20 wt%) in the solvent. Apart from toxic solvents, which are not recommended as green solvents such as dimethylformamide, IPA is commonly used for CNT dispersion [39, 40]. However, IPA has a high evaporation rate, which does not leave much time for the nanomaterials (Ag NWs/CNTs) to penetrate into the fabric; this results in a weak bonding of nanomaterials with the fabric. Figure S2 shows a photograph of the sample's backside after spray coating at 30% pre-strain, revealing that when a DI water/IPA mixture was used as a solvent, the fabric's backside was penetrated by CNTs to a greater depth and turned black. In addition, when the water droplets containing nanomaterials of the same concentration and amount were placed on the fabric, deeper nanomaterial penetration was observed for a DI water/IPA mixture (compared to the case of pure IPA). The black color on the coated surface (i.e. front side) faded because water droplets penetrated into the fabric after being placed thereon (figure S3). In conclusion, IPA allowed for CNT dispersion and DI water allowed for deeper penetration of nanomaterial into the fabric with less evaporation; this resulted in the formation of a robust nanomaterial network within the fabric and reduced temperature variation of the fabric under applied strain (figure S3). A more detailed description of the solvent system and cross-sectional images of the fabric heater prepared using different solvents and pre-strain levels are provided in figure S4.

Figure 1(a) shows a schematic illustration of the fabricated heater, illustrating that the absorption of the coating solution by the fabric was accompanied by nanomaterial transport through the strain-widened yarn gaps and resulted in the deposition of these nanomaterials inside the fabric. After
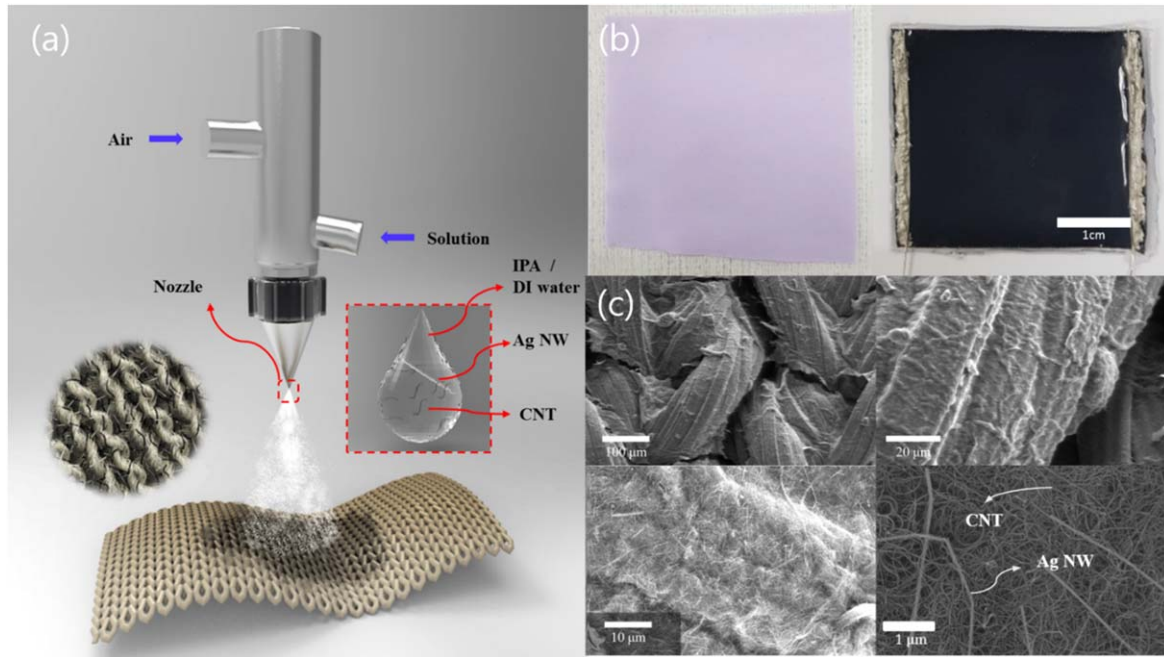
**Figure 1.** Production of a stretchable and flexible fabric heater. (a) Schematic illustration of the spray coating process. (b) Photograph of the fabric substrate before/after nanomaterial deposition. (c) SEM images of deposited Ag NWs and CNTs.
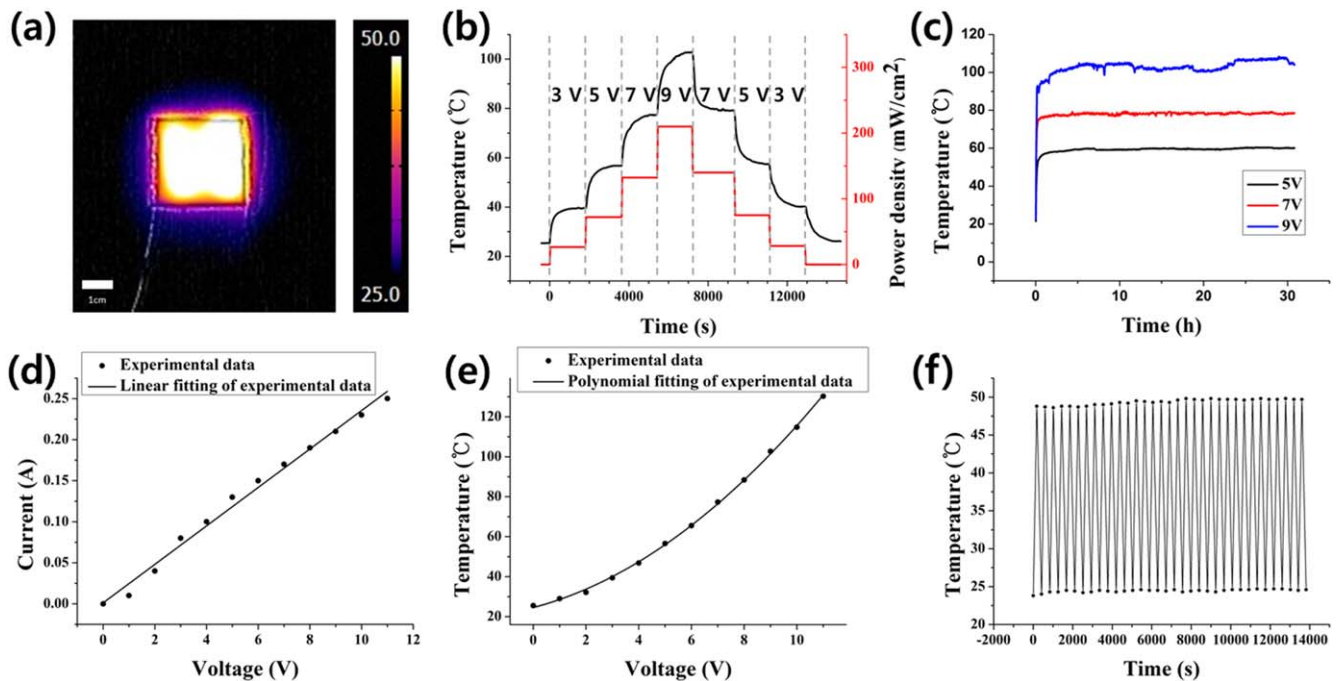


**Figure 2.** Heating performance and electrothermal properties of the stretchable fabric heater. (a) IR thermal image of the heater at an applied voltage of 5 V. (b) Heater response to different electrical voltages and power densities. (c) Temporal change of the heater temperature subjected to different constant DC voltages. (d) *I–V* characteristics of the heater. (e) Dependence of heater temperature on applied voltage. (f) Results of cyclic thermal on/off testing at an input voltage of 4 V (plot shows average temperatures).

coating, a Cu wire electrode was applied to the coated fabric using Ag paste and encapsulated with a highly stretchable (elongation at break = 900%) polymer, Ecoflex 00-30. The high stretchability and wide operation temperature range (−65 °C to 232 °C) of Ecoflex allow the textile and defrosting heaters to be operated without any stretchability degradation.

Although the low thermal conductivity of rubber may result in temperature differences between the polymer surface and inner heating layer (Ag NW/CNT layer), the results of surface temperature measurements were indicative of sufficient wearable heater performance, with further details provided in the electrothermal characteristics part of figure 2.

Figure 1(b) shows the change of fabric color upon spray coating of CNTs + AgNWs and attaching electrodes, and figure 1(c) shows the SEM surface images and reveals the formation of a network of CNTs connecting deposited Ag NWs. Notably, these nanomaterials were well-coated on the fabric without any voids, although CNT agglomeration was observed in some areas; this was ascribed to the imperfect dispersion of CNTs in solution and the aggregation of Ag NWs/CNTs during drying. Likewise, nanomaterials can also aggregate as a whole, resulting in the formation of large cracks when strain is applied. Thus, intentional cracking during the drying process prevented the formation of large Ag NW/CNT aggregates. As shown in figure S5, the aggregation of Ag NW/CNT resulted in the formation of large cracks under applied strain if it was dried without intentional cracking.

### 3.2. Effects of the Ag NW:CNT ratio

The Ag NW:CNT weight ratio was optimized to fabricate a high-performance fabric heater with low sheet resistance, robust structure, flexibility, and a stable nanomaterial network. The optimization result of Ag NW:CNT weight ratio is shown in table 1.

When the coating solution contained only Ag NWs (entry 1), no current flowed between the electrodes as these nanowires were not connected in a network. However, when the coating solution contained only CNTs (entry 5), a relatively high sheet resistance ($82 \, \Omega \, sq^{-1}$) was obtained, and the high degree of CNT aggregation resulted in cracking upon strain application. Thus, it was concluded that the inclusion of both nanomaterials is required for the optimal heater performance. CNTs have a lower density than Ag NWs, implying that for the same total weight of nanomaterials loaded, the volume of the substrate filled with conductive nanomaterials increases with increasing CNT:Ag NW weight ratio. Moreover, the use of CNTs solves the problem of poor adhesion of Ag NWs to the fabric owing to the nonuniformity of its surface. It is worth mentioning that more Ag NWs were observed on the fabric surface in the case of entry 2 than in the case of entry 1, despite the concentration of Ag NWs in the coating solution being lower in the former case. Thus, it can be presumed that many Ag NWs flow out with the solvent unless a trapping network of CNTs is formed during spray coating. From this experiment, preferred solution composition affording high conductivity and stability was found to correspond to entry 2. Typically, Ag NW/CNT hybrid films are fabricated using Ag NWs as the main material to ensure the electrical conductivity and CNTs as a secondary material for the structural stability (Ag NWs:CNTs = 1:1, w/w) [12, 41]. In this study, we found that the nonuniform surface morphology and breathability of the fabric also necessitated the use of similar amounts of CNTs to those of AgNWs (i.e. Ag NW content = CNT content = 0.02 wt%) to form a stable network. The stretchable fabric heater prepared by spray coating 45 ml of the optimum-composition Ag NW/CNT solution featured a low sheet resistance of $22 \, \Omega \, sq^{-1}$ and high

stretchability (∼50% strain; defined as the maximum tensile strain at which the original resistance was restored even after 10 000 cyclic strain tests).

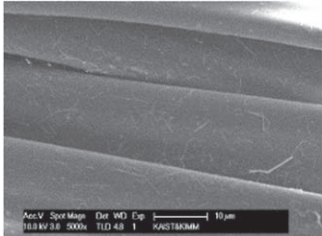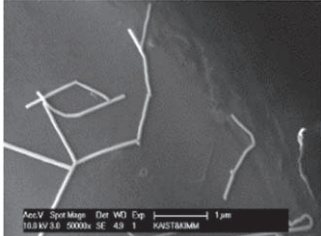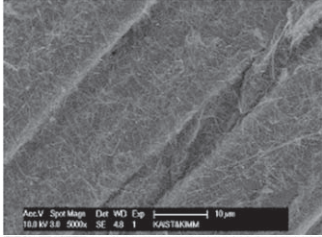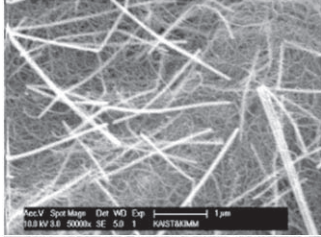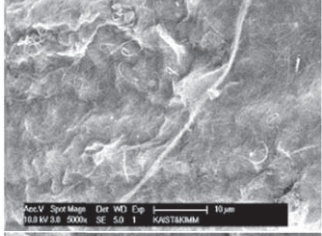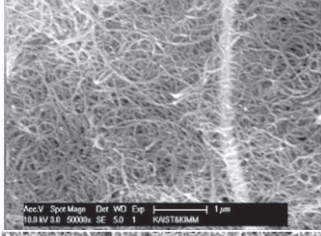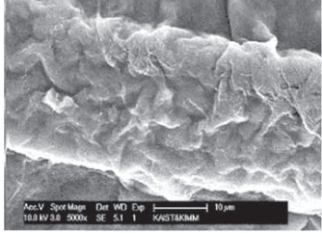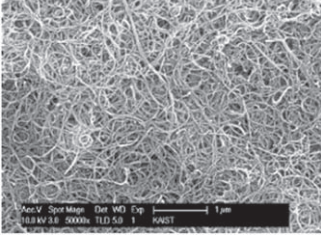### 3.3. Electrothermal characteristics of the fabric heater
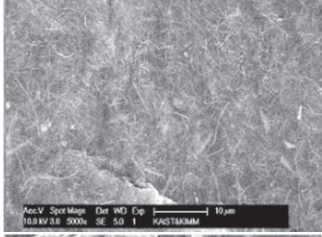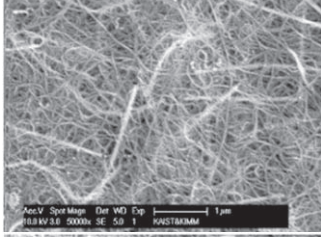
Figure 2 shows the electrothermal properties of the stretchable fabric heater (central heating zone area = 3 cm × 3 cm) prepared under optimal condition explained in section 3.1. The IR image obtained at an input DC bias voltage of 5 V is shown in figure 2(a), while the results of elastomer surface temperature and power consumption are provided in figure 2(b). The latter figure demonstrates that the fabricated heater exhibited a relatively lower power consumption (26.6–72.2 mW cm$^{-2}$ for 35 °C–55 °C) than those reported previously [29] allowing typical operating temperatures of 35 °C–55 °C to be easily reached at low driving voltages of 3–5 V under overall power consumptions of 239–650 mW. Additionally, stable temperature (56.7 °C ± 0.5 °C at 5 V, 78.3 °C ± 1.5 °C at 7 V) could be maintained for more than 30 h without nanomaterial failure (figure 2(c)), and the heater resistance (∼42 Ω) maintained almost constant during heating (figure 2(d)). Although Ag NWs are known to react with oxygen or sulfur-containing gases in the ambient, leading to the failure by oxidation or sulfurization [42–44], it is presumed that the protective coating by Ecoflex provided Ag NWs with higher resistance to these failures in this study. The voltage-dependent temperature increase could be well modeled using the theoretical relationship of $Q = V^2/R$, where $Q$ is the power dissipated in the heater, $V$ is the input voltage, and $R$ is the heater resistance (figure 2(e)).

Moreover, the on/off cyclic test at an applied input DC bias voltage of 4 V revealed a stable behavior of the heater (figure 2(f)). When considered together, the abovementioned results demonstrate an excellent electrothermal performance of the fabricated heater.

### 3.4. Electromechanical characteristics of the fabric heater

In order for the stretchable heaters to be practically applicable, they should maintain consistent performance under various mechanical deformations and exhibit excellent fatigue resistance. Therefore, the fabricated heater was subjected to electromechanical characterization tests (figure 3). The fabric of the weft-knitted structure used in this study had a wale and course directions according to the woven direction, with the course direction having a larger maximum elongation than that of the wale direction due to the woven structure of weft-knitted fabric. For the fabric employed in this work, plastic deformation, which indicates maximum stretchability of the fabric itself, occurred at about 50%–70% strain in the course direction and at 30%–50% strain in the wale direction. Figure 3(a) shows the heater temperature change for each direction under applied strain. The observed temperature change (⩽18%) within 30% strain in each direction can be regarded as a small value in wearable applications [45]. This behavior was ascribed to the fact that Ag NWs/CNTs could penetrate well into the fabric

**Table 1.** Effect of the CNT:Ag NW weight ratio on the fabric heater performance.

| # | SEM image (5000×) | SEM image (50 000×) | CNT/ Ag NW (wt%) | Amount of coating solution (ml) | Average sheet resistance ($\Omega$ sq$^{-1}$) | Cracks after stretching (O: occurred, X: did not occur) |
|---|---|---|---|---|---|---|
| 1 |  |  | 0.00/ 0.04 | 35 | $\infty$ | X |
| 2 |  |  | 0.01/ 0.03 | 35 | $157 \pm 28$ | X |
| 3 |  |  | 0.02/ 0.02 | 35 | $34 \pm 4$ | X |
| 4 |  |  | 0.03/ 0.01 | 35 | $47 \pm 12$ | O |
| 5 |  |  | 0.04/ 0.00 | 35 | $82 \pm 5$ | O |

and create a conductive layer that allowed current flow (via a serpentine route) even when strain was applied (further details are provided in figure S3). To ensure reliability, a resistance change experiment (figure 3(b)) and a cyclic strain test (figure 3(c)) were also performed for the course direction. In all tensile tests, the direction of applied voltage was parallel to that of the applied strain. At 70% strain, the fabric experienced plastic deformation and took a long time to recover; consequently, a permanent resistance increase was observed when the cyclic test was performed at 70% strain. In contrast, negligible resistance changes (within 5%) were observed during 10 000 cycles at 30% and 50% strains, i.e. at strain values that

can be encountered during practical applications; this demonstrated that the fabricated heater exhibits excellent mechanical characteristics. Mechanical robustness against folding and rolling, which is one of the most important characteristics of wearable electronics, was investigated as shown in figures 3(d) and (e). Notably, folding and rolling resulted in only negligible resistance change (within 5%), and IR imaging of folded and rolled states revealed that their temperature equaled that of the initial state. Thus, the high flexibility of Ecoflex 00-30 (Young's modulus $\approx 34.8$ kPa) and the stable structures of the Ag NW/CNT network resulted in excellent foldability and rollability of the heater.
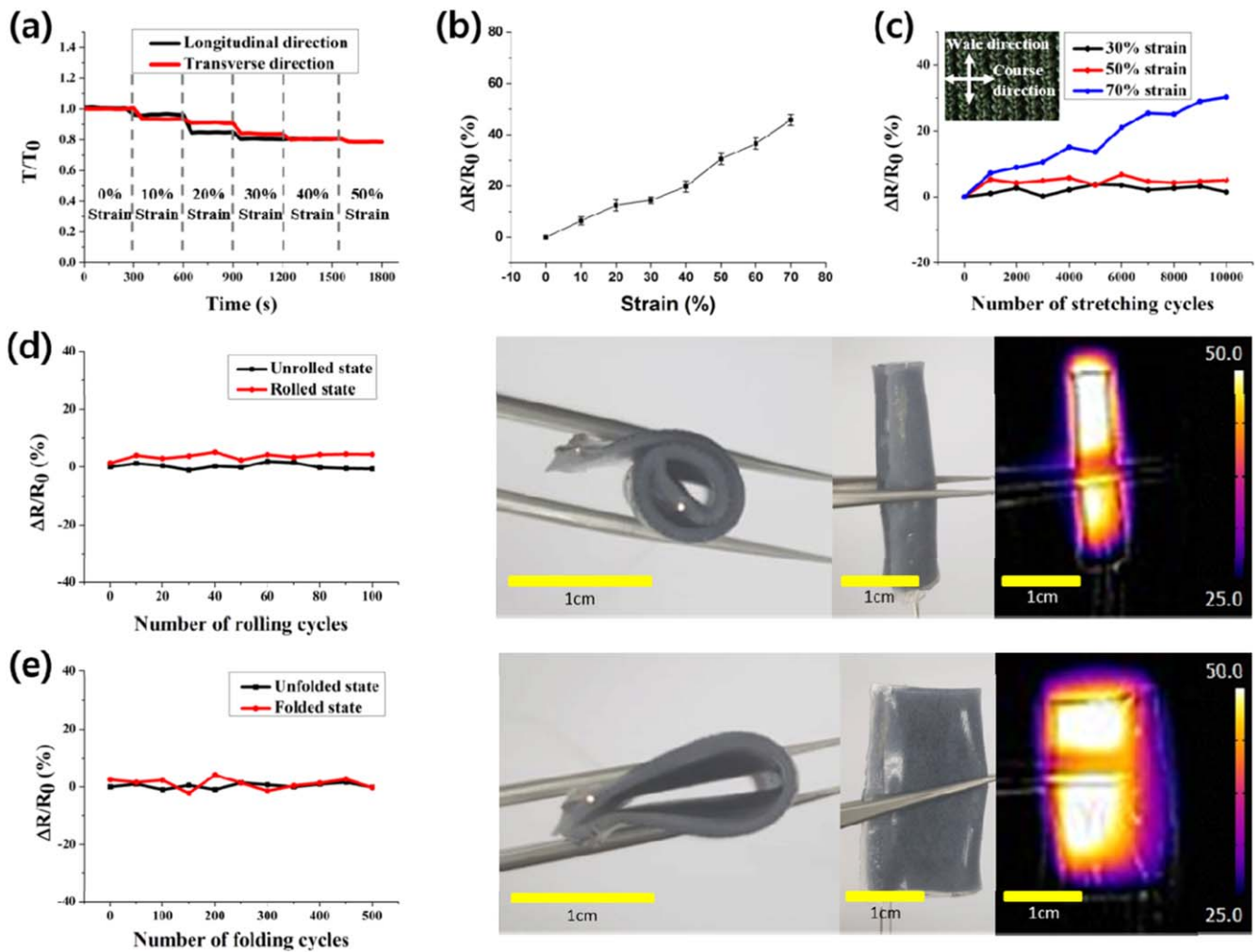
**Figure 3.** Mechanical and electrical properties of the stretchable fabric heater. (a) Change of temperature with time during stretching in different directions. (b) Change of electrical resistance with applied strain. (c) Effect of maximum strain on heater's thermal stability during repeated stretching. Photographic/IR thermal images and resistance changes during repeated (d) rolling and (e) folding tests. Except for '(a)', strain was applied in the transverse (course) direction, and input voltage of 5 V was used. $R_0$ ($\approx 42\ \Omega$) is the initial resistance of the heater and $T_0$ ($\approx 55\ °C$) is the initial temperature of the heater under input voltage of 5 V. The transverse and longitudinal directions are the course and wale directions, respectively, in (a) and (c).

### 3.5. Demonstration of wearable and defrosting heaters

To demonstrate the practical utility of the developed approach, we applied it to fabricate wearable heaters and portable defrosting heaters (figure 4).

First, we demonstrated that the employed fabrication process is applicable to a wide range of commercial textiles by using cotton gloves as a model substrate for Ag NW/CNT deposition. After Cu electrodes were fitted using Ag paste and Ecoflex 00-30 was applied as a cover polymer, Joule heating caused by the input voltage application occurred only in the nanomaterial-coated part. IR imaging showed that the heater worked well at an input DC voltage of 8 V, and a low-temperature manikin was used to clearly distinguish the heated part (figure 4(a)). Figure 4(c) shows the effect of applied voltage on the temperature change of the glove heater, revealing that the driving voltage of the heater formed on fingers exceeded that of the heater formed on the back of the hand. This finding was ascribed to the fact that the heating

areas of these two heaters were different and the surface morphology of the finger part featured numerous curved areas, highlighting the need for further optimization of the fabrication process for the substrates with different surface morphologies and three-dimensional curvatures. Under identical conditions (coating degree, drying time, etc), the performance of the glove heater was different from that of the previously described model heater; this is ascribed to the corresponding differences in employed materials and surface morphology. However, this demonstration showed the feasibility of direct heater fabrication on any commercial fabric. To the best of authors' knowledge, this work is the first report of a stretchable heater prepared by direct coating of conductive nanomaterials onto a fabric without the additional attachment of heaters or sewing threads.

Second, the performance of the portable defrosting heater was evaluated by placing frosted glass on the heater and measuring the fraction of the frosted area as a function of time at different power densities and maintaining an ambient
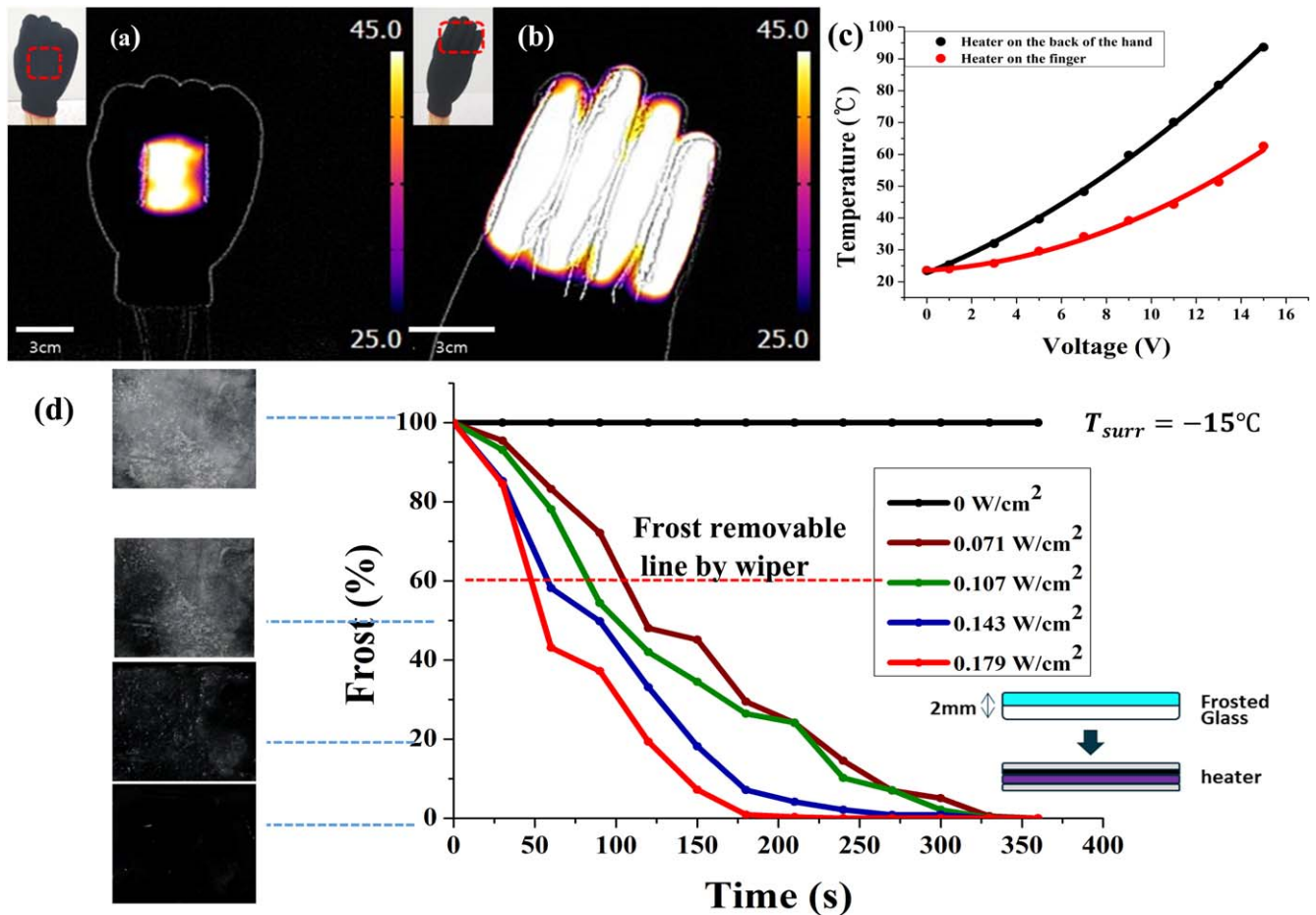
**Figure 4.** Applications of the developed spray coating technique to the fabrication of wearable heaters and defrosting heaters. Photographic/ IR thermal images of a heater produced by coating of Ag NWs/CNTs on (a) the backside and (b) fingers of a cotton glove. (c) Dependence of glove heater temperature on applied voltage. (d) Effect of applied power density on defrosting performance.

temperature of −15 °C (figure 4(d)). No change of frosted area fraction was observed at the reference temperature, whereas sudden defrosting (50%–80%) occurred when a voltage was applied. In the initial 80%–100% frost range, no significant change of frosted area fraction was observed as the glass layer was just heated. In the 50%–80% frost range, heat was transferred directly from the glass to the frosted area via thermal conduction, resulting in rapid defrosting. Subsequently, the defrosting rate decreased as the water layer produced by frost removal from the glass surface reduced the efficiency of further heat transfer. However, at a frosting degree of <60%, the amount of generated water was sufficient for the remaining frost to be easily removed by a screen wiper or under the action of gravity. Thus, a power supply of at least 71 mW cm$^{-2}$, which can be easily provided by a car battery or a portable battery pack, was sufficient to remove frost within 120 s after the attachment of the heater to the glass. The presence of a protective polymer coating prevented fabric wetting by the produced water, and thus precluded wetting-induced changes of heater performance, and the enhanced rollability and foldability achieved in this study were concluded to be well suited for the fabrication of practical foldable heaters.

## 4. Conclusion

In this study, we used spray coating of Ag NW/CNT nanocomposites to prepare a fabric heater with high stretchability (up to 50% without performance degradation after 10 000 cycles) and low sheet resistance (22 Ω sq$^{-1}$), demonstrating the practical applicability of the developed technique to the fabrication of wearable heaters and portable defrosting heaters. The unique characteristic of the employed breathable fabric, optimization of Ag NW/CNT compositions, and the utilization of DI water/IPA mixture allowed for the deep penetration of Ag NWs/CNTs and resulted in high mechanical robustness, stretchability, flexibility, rollability, and foldability. The developed spray coating process was shown to be applicable to the fabrication of wearable electrodes or electronic platforms, and the excellent mechanical and thermal characteristics of the produced fabric heater implied that the adopted approach is well suited for electrothermal actuation or thermotherapy. Therefore, the present study provides a new direction of research in the field of wearable devices and can be viewed as a benchmark for subsequent research.

## Acknowledgments

## ORCID iDs

Junho Jeong ● https://orcid.org/0000-0002-5631-3626
Inkyu Park ● https://orcid.org/0000-0001-5761-7739

## References

[1] Yetisen A K *et al* 2016 *ACS Nano* **10** 3042–68
[2] Weng W, Chen P, He S, Sun X and Peng H 2016 *Angew. Chem., Int. Ed.* **55** 6140
[3] Yeon C, Kim G, Lim J W and Yun S J 2017 *RSC Adv.* **7** 5888
[4] Doganay D, Coskun S, Genlik S P and Unalan H E 2016 *Nanotechnology* **27** 435201
[5] Cheng Y, Zhang H, Wang R, Wang X, Zhai H, Wang T, Jin Q and Sun J 2016 *ACS Appl. Mater. Interfaces* **8** 32925
[6] Zhang M, Wang C, Liang X, Yin Z, Xia K, Wang H, Jian M and Zhang Y 2017 *Adv. Electron. Mater.* **3** 1700193
[7] Gupta R, Rao K D M, Kiruthika S and Kulkarni G U 2016 *ACS Appl. Mater. Interfaces* **8** 12559
[8] Pillai S K R, Wang J, Wang Y, Sk M M, Prakoso A B, Rusli and Chan-Park M B 2016 *Sci. Rep.* **6** 38453
[9] Kim C-L, Jung C-W, Oh Y-J and Kim D-E 2017 *NPG Asia Mater.* **9** e438
[10] Jing M-X, Han C, Li M and Shen X Q 2014 *Nanoscale Res. Lett.* **9** 588
[11] Lordan D, Burke M, Manning M, Martin A, Amann A, O'Connell D, Murphy R, Lyons C and Quinn A J 2017 *ACS Appl. Mater. Interfaces* **9** 4932
[12] Lee Y R, Kwon H, Lee D H and Lee B Y 2017 *Soft Matter* **13** 6390
[13] Kang J, Kim H, Kim K S, Lee S-K, Bae S, Ahn J-H, Kim Y-J, Choi J-B and Hong B H 2011 *Nano Lett.* **11** 5154
[14] Zhou R, Li P, Fan Z, Du D and Ouyang J 2017 *J. Mater. Chem. C* **5** 1544
[15] Jung D, Kim D, Lee K H, Overzet L J and Lee J S 2013 *Sensors Actuators* A **199** 176
[16] Liu P, Zhou D, Wei Y, Jiang K, Wang J, Zhang L, Li Q and Fan S 2015 *ACS Nano* **9** 3753
[17] Jang H-S, Jeon S K and Nahm S H 2011 *Carbon* **49** 111
[18] Lan W *et al* 2017 *ACS Appl. Mater. Interfaces* **9** 6644
[19] Walia S, Gupta R, Rao K D M and Kulkarni G U 2016 *ACS Appl. Mater. Interfaces* **8** 23419
[20] An B W, Gwak E J, Kim K, Kim Y-C, Jang J, Kim J-Y and Park J-U 2015 *Nano Lett.* **16** 471
[21] Ha B and Jo S 2017 *Sci. Rep.* **7** 11614
[22] Jang J, Hyun B G, Ji S, Cho E, An B W, Cheong W H and Park J-U 2017 *NPG Asia Mater.* **9** e432
[23] Jo H S, An S, Lee J-G, Park H G, Al-Deyab S S, Yarin A L and Yoon S S 2017 *NPG Asia Mater.* **9** e347
[24] Kim D, Zhu L, Jeong D-J, Chun K, Bang Y-Y, Kim S-R, Kim J-H and Oh S-K 2013 *Carbon* **63** 530
[25] Hong S *et al* 2015 *Adv. Mater.* **27** 4744
[26] Wang R, Xu Z, Zhuang J, Liu Z, Peng L, Li Z, Liu Y, Gao W and Gao C 2017 *Adv. Electron. Mater.* **3** 1600425
[27] Zhou J, Mulle M, Zhang Y, Xu X, Li E Q, Han F, Thoroddsen S T and Lubineau G 2016 *J. Mater. Chem.* C **4** 1238
[28] Zhong X, Wang R, Yangyang W and Yali L 2013 *Nanoscale* **5** 1183
[29] Ilanchezhiyan P, Zakirov A S, Kumar G M, Yuldashev S U, Cho H D, Kang T W and Mamadalimov A T 2015 *RSC Adv.* **5** 10697
[30] Zhang L, Baima M and Andrew T L 2017 *ACS Appl. Mater. Interfaces* **9** 32299
[31] Opwis K, Knittel D and Gutmann J S 2012 *Synth. Met.* **162** 1912
[32] Yu X, Su X, Yan K, Hu H, Peng M, Cai X and Zou D 2016 *Adv. Mater. Technol.* **1** 1600009
[33] Atwa Y, Maheshwari N and Goldthorpe I A 2015 *J. Mater. Chem.* C **3** 3908
[34] Hao D, Xu B and Cai Z 2018 *J. Mater. Sci.: Mater. Electron.* **29** 9218–26
[35] Wang J-T, Hsu C-C, Chen C-M and He J-L 2013 *Thin Solid Films* **528** 247
[36] Tokuno T, Nogi M, Jiu J and Suganuma K 2012 *Nanoscale Res. Lett.* **7** 281
[37] Lee J, Woo J Y, Kim J T, Lee B Y and Han C-S 2014 *ACS Appl. Mater. Interfaces* **6** 10974
[38] Ramasamy E, Lee W J, Lee D Y and Song J S 2008 *Electrochem. Commun.* **10** 1087–9
[39] Byrne F P, Jin S, Paggiola G, Petchey T H, Clark J H, Farmer T J, Hunt A J, McElroy C R and Sherwood J 2016 *Sustain. Chem. Process.* **4** 7
[40] Soltani K F, Zabihi F, Xie Y and Eslamian M 2015 Conductive CNT-and graphene-doped PEDOT:PSS yhin films fabricated by ultrasonic spray coating *13th Triennial Int. Conf. on Liquid Atomization and Spray Systems*
[41] Stapleton A J, Afre R A, Ellis A V, Shapter J G, Andersson G G, Quinton J S and Lewis D A 2013 *Sci. Technol. Adv. Mater.* **14** 035004
[42] Khaligh H H and Goldthorpe I A 2013 *Nanoscale Res. Lett.* **8** 2
[43] Elechiguerra J L, Larios-Lopez L, Liu C, Garcia-Gutierrez D, Camacho-Bragado A and Yacaman M J 2005 *Chem. Mater.* **17** 6042
[44] Liu B T and Huang S X 2014 *RSC Adv.* **4** 59226
[45] Wang Y, Wang L, Yang T, Li X, Zang X, Zhu M, Wang K, Wu D and Zhu H 2014 *Adv. Funct. Mater.* **24** 4666–70